

Multiphonon relaxation of rare-earth ions in oxide glasses*

C. B. Layne, W. H. Lowdermilk, and M. J. Weber

Lawrence Livermore Laboratory, University of California, Livermore, California 94550

(Received 14 December 1976)

Nonradiative decay of excited rare-earth ions by multiphonon emission has been investigated in a series of oxide glasses. Various rare-earth electronic levels were selectively excited by short-duration laser pulses and multiphonon relaxation rates were determined from measurements of fluorescence rise and decay times. Time resolution for fluorescence measurements was 3 nsec, so excited states were probed for which the decay was predominantly nonradiative. Excited states of Nd^{3+} , Er^{3+} , and Tm^{3+} with energy gaps to the next-lower J state ranging from 1300 to 4700 cm^{-1} were studied. The multiphonon relaxation rates for each glass investigated exhibited an approximately exponential dependence on energy gap. Evidence of breakdown of this dependence was observed in the region of small energy gaps. The measured temperature dependences of the decay rates establish that the relaxation occurs predominantly by excitation of the highest-frequency vibrations associated with stretching modes of the glass network former. Borate, silicate, phosphate, germanate, and tellurite glasses were studied. From Raman spectra, the highest-frequency vibrations for these glasses ranged from 700 to 1400 cm^{-1} . The corresponding multiphonon relaxation rates for a given energy gap differed by three orders of magnitude. The strength of the ion-phonon coupling was found to be approximately equal for all glasses.

I. INTRODUCTION

Excited electronic states of rare-earth ions in solids can decay nonradiatively by exciting lattice vibrations. When the energy gap between the excited state and the next-lower state is larger than the maximum phonon energy in the material, emission of several phonons is required to conserve energy. Relaxation by multiphonon processes is well established from studies of rare earths in crystals.¹ These results demonstrate that for high-order processes (≈ 3 phonons), the decay rate is determined predominantly by the number of phonons required to bridge the energy gap. Since the highest-energy phonons can conserve energy in the lowest-order process, they are most important in the relaxation. Because of the different vibrational spectra, the rate of multiphonon processes is host dependent. The dependence on specific rare-earth or electronic states involved is negligible unless there are strong selection rules.

Multiphonon processes of rare earths in glasses arise from the same general physical processes as in crystals. The rare earth has oxygen or other anions as nearest neighbors. The vibrations of these and more distant ions contribute to the fluctuating Stark field which induces nonradiative transitions, as in the case of crystals. There are, however, several differences in decay properties between glasses and crystals.

First, the spectrum and nature of vibrations in amorphous materials are different and their detailed understanding is still incomplete. For multiphonon relaxation, one is interested in the

highest frequency phonons. In glasses, these are the stretching vibrations of the glass network former polyhedron, a "molecular" vibration that is localized and weakly coupled to the network as a whole. In addition to these vibrations, there is a spectrum of lower-frequency modes.

A second difference is the energies of the highest-frequency vibrations in glasses. For oxide glasses, these range from 700 to 1400 cm^{-1} and are much higher than the highest optical-mode frequencies in most oxide and halide crystals commonly used as rare-earth hosts. Therefore, for a given rare-earth excited state and for comparable ion-phonon coupling strengths, a lower-order multiphonon process in such glasses will be capable of bridging the energy gap. The resulting relaxation is faster. Since the radiative decay rates for rare-earth ions in crystals and glasses are the same order of magnitude, the large nonradiative decay probability in oxide glass leads to low fluorescence quantum efficiency. This is reflected in the smaller number of fluorescing states observed for rare earths in glasses as compared to most crystals. This may not be true for the crystalline analogs of borate, phosphate, and silicate glasses where the highest-frequency vibrations are similar. This feature has consequences for the experimental approach, detection sensitivity, and time resolution to be employed for studying multiphonon relaxation in glass.

Finally, rare earths in glass occupy nonequivalent sites which arise from different crystal-field symmetries and strengths. Depending upon the type of network modifier ions present, there are site-to-site variations in (i) the Stark splitting,

as evident in the inhomogeneously broadened optical absorption and emission lines; and (ii) the radiative transition probability, as evident in the nonexponential fluorescence decays. By using fluorescence line narrowing techniques, the variations in these properties have been investigated.² In the normal optical experiment using a broadband excitation source, some effective combination of sites is observed. Multiphonon decays in glasses are expected to show nonexponential character due to site-to-site variations in the energies and coupling strengths of the network vibrations.

The first quantitative studies of rare-earth multiphonon relaxation in glasses were conducted by Reissfeld's group at Hebrew University.³ Several rare earths and oxide glasses were examined, but due to experimental considerations it was not possible to study the same transition (energy gap) in all glasses, nor all transitions in the same glass. Also, determination of multiphonon rates depended strongly on the accuracy of calculated radiative rates. The results did, however, reveal a dependence of the nonradiative decay rate on energy gap, host, and temperature.

In this paper we investigate multiphonon relaxation of several different rare-earth ions and electronic states in a series of five oxide glasses with a wide range of vibrational frequencies. By using improved time-resolution and selective excitation techniques, it was possible to study more excited states and a greater range of energy gaps than have been measured previously. In addition, most measurements of lifetimes were made for cases where the probability for nonradiative decay was very much greater than for radiative decay; hence, the latter could be neglected. In the few cases where this approximation was not valid, radiative probabilities were estimated using Judd-Ofelt intensity parameters.⁴

In Sec. II we review the theory of multiphonon relaxation as applied to glasses. The experimental approach and apparatus are described in Sec. III. Measured relaxation rates for individual rare-earth ions in different glasses are presented in Sec. IV, including measurements of the temperature dependence of the rates and the Raman spectra of the glasses. Our conclusions are summarized in Sec. V.

II. THEORY OF MULTIPHONON PROCESSES

The $4f$ electrons of the trivalent rare earths are weakly coupled to their environments through the crystal field of the surrounding ions. For a one-phonon direct process, lattice vibrations modulate the crystal field, causing transitions between rare-earth electronic levels separated by

energies equal to that of the lattice mode. When the energy difference between adjacent levels exceeds the maximum energy in the crystal phonon spectrum, a less probable, higher-order process is required to bridge the energy gap. Kiel⁵ developed a theory of multiphonon relaxation in crystals, which was subsequently extended by Riseberg and Moos.⁶ There are three predictions of the theory of multiphonon relaxation: the exponential dependence of multiphonon rates on the energy gap, the importance of the highest-energy phonons in the material, and finally, the temperature dependence of multiphonon decay. Riseberg and Weber¹ have recently reviewed multiphonon decay in crystals, including the extensive experimental data supporting the theory.

Several different approaches to the theory of multiphonon relaxation, including those of Miyakawa and Dexter,⁷ Fischer,⁸ Fong and co-workers,⁹ and Struck and Fonger,¹⁰ yield similar predictions of an approximately exponential dependence of the rate on energy gap. Predictions of temperature dependence differ somewhat from the results of Kiel⁵ and of Riseberg and Moos.⁶ None of these approaches actually calculates the matrix elements for the transitions and the resulting rates. Kiel's perturbation approach is used here because of the clear connection between the rate calculation and the physical processes involved.

Application of the multiphonon theory to glasses requires consideration of the vibrational properties of amorphous solids. According to present theories of glass structure, oxide glasses of the type considered here are formed from networks of glass-forming ions such as Si, B, P, Ge, or Te which are strongly linked by bridging oxygen ions.¹¹ Distinct structural units such as SiO_4 tetrahedra exist in the glasses with random orientations. Adding network modifiers such as alkali or alkaline earth ions breaks up the three-dimensional network, thereby introducing nonbridging oxygens. The vibrations involving the network modifiers are between two and four times lower in frequency than the vibrations of the network formers.¹²

Bell and co-workers,¹³ Su and co-workers,¹⁴ and Bates¹⁵ have attempted to calculate the vibrational motion of the network in simple glasses, using a model for the network of ionic masses with appropriate bond strengths. Solving for the modes of vibration resulted in fair agreement with observed Raman and infrared spectra. They found that the high-energy vibrations of the glass network involve localized vibrations of the glass-forming units (SiO_4 , for example), with frequencies near that of the Si-O bond stretching vibration. The high-energy modes that couple to the rare-earth ion in a glass are best approximated by a few

independent oscillators (for instance, SiO_4 tetrahedra) that surround the ion and are only weakly coupled to the other oscillators in the glass. This molecular model is similar to the Einstein model for the vibrational spectrum of a solid. Brawer¹² has included the coupling of the high-energy oscillators in his formulation of the theory of vibrational spectra of network glasses, and he has shown that this coupling is weak.

The lack of symmetry in a glass and the molecular character of the high-energy vibrations lead to the present approach to multiphonon theory for glasses. The overriding importance of the highest-energy vibrational modes observed in the case of crystals leads us to consider only these modes in glasses, a premise that must be verified by comparison with experiment. The formulation of multiphonon theory for glasses differs from Kiel's formulation for crystals in the following way. In a glass, a few independent oscillators (glass-forming polyhedra such as SiO_4) are coupled to the ion; whereas, for a crystal, Kiel considered the normal modes of the rare earth oscillating relative to its nearest neighbors and then formally expanded these oscillators in terms of the lattice modes. Calculations of transition rates based upon this expansion are prohibitively difficult.⁵

Since the rare-earth ion is weakly coupled to the glass network, the system wave function $|\chi\rangle$ may be conveniently expressed as a product of the ion electronic state $|\psi_e\rangle$ and the network normal vibrational modes each characterized by its occupation number n_i :

$$|\chi\rangle = |\psi_e\rangle \prod_i |n_i\rangle. \quad (1)$$

Interaction between the rare-earth ion and the network is due to modulation of the crystal field by the lattice vibrations. With a simple point charge model for the glass network, the interaction Hamil-

tonian may be expanded in a Taylor series around the equilibrium positions

$$H_{\text{int}} = V_0 + \sum_i V_i Q_i + \sum_{ij} V_{ij} Q_i Q_j + \dots, \quad (2)$$

where Q_i is a network normal mode coordinate, V_0 is the static crystal field, and the coefficients V_i, V_{ij} are simply derivatives of the crystal field with respect to the normal modes:

$$V_i = \frac{\partial V}{\partial Q_i}, \quad V_{ij} = \frac{\partial^2 V}{\partial Q_i \partial Q_j}, \quad \text{etc.} \quad (3)$$

The rate for a one-phonon transition involves matrix elements of those modes that couple to the ion through the second term in Eq. (2) and also conserve energy between the initial electronic state ψ_a and the final state ψ_b . This rate is formally given by

$$W_1 = \frac{2\pi}{\hbar} \left| \sum_i \langle \psi_b | V_i | \psi_a \rangle \prod_j \langle n_j | Q_i | n_j \rangle \prod_{j \neq i} |n_j\rangle \right|^2. \quad (4)$$

As in the case of crystals, the system is too complex for actual evaluation of the matrix elements in Eq. (4).

When the initial and final electronic states are separated in energy by an amount greater than the highest phonon energy in the glass, the perturbation calculation must be done in higher order to allow emission of two or more phonons. Multiphonon emission can result from the second term in Eq. (2) taken in high order of the perturbation calculation or from a higher-order term in the expansion taken in a lower order of the perturbation calculation.

Taking the single-phonon term in the expansion of the potential in a p -order perturbation calculation, the rate for a transition across an energy gap ΔE accompanied by emission of p phonons all of energy $\hbar\omega = \Delta E/p$ is given by

$$W_p = \frac{2\pi}{\hbar} \left| \left(\frac{\hbar}{2M\omega} \right)^{p/2} \sum_{\substack{i, j, \dots, p \\ = 1, 2, \dots, m}} (n_i + 1)^{p/2} \frac{\langle \psi_b | V_i | \psi_{a,b} \rangle \langle \psi_{a,b} | V_j | \psi_{a,b} \rangle \dots \langle \psi_{a,b} | V_p | \psi_a \rangle}{(E_a - E_{a,b} - \hbar\omega)(E_a - E_{a,b} - 2\hbar\omega) \dots (E_a - E_{a,b} - [p-1]\hbar\omega)} \right|^2, \quad (5)$$

where M is the reduced mass. The number of oscillators m coupled to the ion is given by the number of nearest-neighbor glass-forming units (between six and eight for these oxides) times the number of high-frequency modes in each unit that couples to the ion. For small m , terms in Eq. (5) involving multiple excitation of a single mode $(n+1)(n+2)\dots$ will result. If m is approximately 10 or larger, as assumed here, the relaxation is dominated by terms involving $(n+1)^p$, as shown in Eq. (5).

The subscript a, b on the intermediate states indicates that the 2^{p-1} possible different sequences of intermediate electronic states must be included in the sum. The simplifying assumption is made that each of the matrix elements in Eq. (5) can be replaced by an average value $|\langle a | V' | b \rangle|$. Then, the multiphonon transition rate is

$$W_p = \frac{2\pi}{\hbar} \left(\frac{\hbar}{2M\omega} \right)^p (n+1)^p 2^{2(p-1)} m^{2p} \frac{|\langle a | V' | b \rangle|^{2p}}{(\hbar\omega)^{2(p-1)}}. \quad (6)$$

The sum over intermediate electronic states when squared gives $2^{2(p-1)}$ terms, and for each of these there are m^{2p} terms from the square of the sum over coupled phonon modes.

The temperature dependence of the multiphonon rate arises from its dependence on the Bose-Einstein occupation number of the phonon mode

$$n(T) = (e^{\hbar\omega/kT} - 1)^{-1}. \quad (7)$$

For a p -order process, the temperature dependence of $(n+1)^p$ identifies the order of the process and the energy of the phonons $\hbar\omega$.

Multiple excitation of a single mode results in a different temperature dependence: $(n+1)(n+2)\dots$ in place of $(n+1)^p$. This difference may be observable in cases where m is small; for instance, in a glass where water accounts for rapid relaxation of a rare-earth excited state.

The dependence of a multiphonon rate on the energy gap to be bridged results from comparing the rate for a p -phonon process with that for a $p-1$ phonon decay. With the same glass network, $\hbar\omega$ and m are the same for W_p and W_{p-1} . Assuming the average matrix element to be the same for p - and $(p-1)$ -order processes, the ratio of W_p to W_{p-1} is

$$W_p/W_{p-1} = (\hbar/2M\omega)(n+1)4m^2|\langle a|V'|b\rangle|^2/(\hbar\omega)^2. \quad (8)$$

Since the perturbation is weak,

$$W_p/W_{p-1} = \epsilon \ll 1. \quad (9)$$

This result leads to the following exponential dependence of the rate on energy gap⁶:

$$W_p = W_0 \epsilon^p = W_0 \exp[\ln(\epsilon)/\hbar\omega] \Delta E. \quad (10)$$

Considering the dependence of W_p on the phonon occupation number from Eq. (6), the rate for a p -order multiphonon decay is

$$W_p = C\{n(T)+1\}^p \exp(-\alpha\Delta E), \quad (11)$$

where $\alpha = -\ln(\epsilon)/\hbar\omega$ and the constant C depends on the host. This result expresses both the exponential dependence of multiphonon relaxation rate on the energy gap across which the decay takes place and the explicit temperature dependence.

The weakest approximation in this derivation is the assumption that the average matrix element $|\langle a|V'|b\rangle|$ is equal for different p and for different electronic states. German and Kiel¹⁷ have observed multiphonon rates in crystals that deviate from the predictions of multiphonon theory when strong selection rules were active. It is clear that variations of ϵ should be expected; but ϵ enters the final result as $\ln(\epsilon)$, which accounts for the insensitivity of the prediction to the exact nature of the ion-phonon coupling.

The validity of Eq. (11) for crystals has been demonstrated for rare-earth energy levels in many hosts. The values of C and α vary from host to host, but for a given host, Eq. (11) is valid to an accuracy of a factor of two or better.¹ The high-energy optical phonons also change from host to host, and this is the primary cause of variations in the observed rates from crystal to crystal.

The results of multiphonon decay measurements in glasses reported here confirm that this theory has predictive value in glasses as well as in crystals, in spite of the differences between the two media. The aspects of multiphonon theory that are directly verified by the experiments reported here are: (i) the exponential dependence of multiphonon rate on energy gap; (ii) the dominance of the the highest-energy phonons and the resulting systematic variation of decay rates with glass composition; and (iii) the temperature dependence of multiphonon decay determined by the thermal population of the highest-energy vibrational modes.

III. EXPERIMENTAL

A. Approach

Multiphonon decay rates were measured using pulsed selective excitation and observation of the fluorescence decay. To illustrate this approach, consider the representative energy-level scheme for rare-earth ions and examples of radiative and nonradiative transitions shown in Fig. 1. If an ion

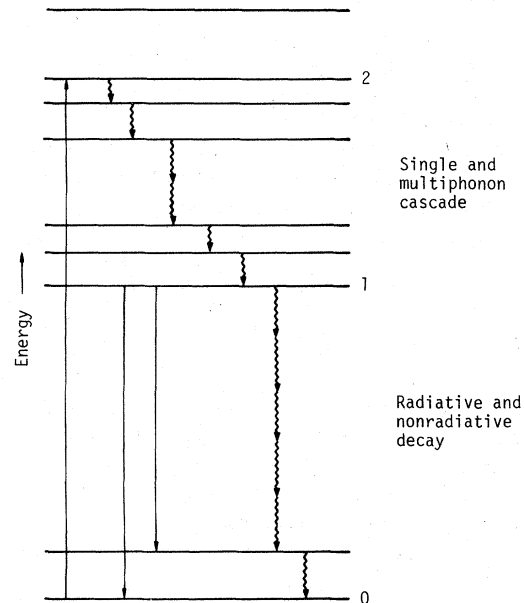


FIG. 1. Representative decay scheme for rare-earth ions in glass. Solid-line and wavy-line transitions denote radiative and nonradiative (phonon-induced) processes, respectively.

is excited to an electronic state with a small energy gap to the next-lower Stark level or nearby J manifold, one-phonon and Raman processes can cause very rapid ($\ll 1$ nsec) nonradiative relaxation. For larger energy gaps, several phonons are required to conserve energy and the decay is much slower. The lifetime τ_a of an excited state a is given by

$$\frac{1}{\tau_a} = \sum_b (A_{ab} + W_{ab}), \quad (12)$$

where A_{ab} and W_{ab} are the radiative and nonradiative transition probabilities from level a to level b , and the summation is over all terminal levels b . Nonradiative processes include, in addition to multiphonon decay, relaxation by direct ion-ion transfer and energy migration to quenching centers. In the experiments reported below, the rare-earth concentrations were small so that nonradiative relaxation by ion-ion interactions was negligible.

The radiative quantum efficiency of a transition $a \rightarrow b$ is defined by

$$\eta_{ab} = A_{ab} / \sum_b (A_{ab} + W_{ab}) = \tau_a A_{ab}. \quad (13)$$

All rare-earth electronic states have some finite radiative transition probability. For levels with small energy gaps to the next-lower level, decay by multiphonon emission is very fast ($W_p \gg A$), so fluorescence is not normally observed. In Fig. 1, the only fluorescing level indicated is the metastable level 1, which has a large energy gap.

The instantaneous fluorescence intensity is proportional to the number of excited ions in the upper state. If ions are initially excited by a short light pulse directly into a fluorescing level such as level 1 in Fig. 1, the fluorescence will decay with a simple, exponential time dependence $\exp(-t/\tau_1)$. The lifetime τ_1 is given by Eq. (12). If, instead, ions are initially excited into a higher-energy level 2, then the time dependence of the fluorescence is described by

$$\phi_1(t) = [W_2 / (W_1 - W_2)] [\exp(-W_2 t) - \exp(-W_1 t)], \quad (14)$$

where $W_1 = \tau_1^{-1}$ and W_2 is the decay rate from level 2, which is assumed to decay only by multiphonon emission to level 1. The fluorescence signal rises and decays with a peak occurring at a time

$$t_p = \frac{\ln(W_2/W_1)}{(W_2 - W_1)}. \quad (15)$$

Thus, by measuring τ_1 and the risetime or peak t_p , the decay rate of a nonfluorescing level can be determined. In an energy-level scheme such as shown in Fig. 1, ions excited into level 2 relax

to level 1 via a level-by-level nonradiative cascade. The time t_p is then dominated by decay across the largest-energy gap in the cascade, which is the rate-limiting step.

The techniques of pulsed selective excitation and fluorescence decay measurements have been applied to study relaxation of rare-earth ions in crystals.¹⁸ The same approach is applied here to determine multiphonon decay rates for rare earths in glasses. As noted previously, because of the higher-energy phonons present in glasses, the multiphonon relaxation rates for a given energy gap are faster in glasses than in crystals. The radiative probabilities A for trivalent rare earths, however, are the same order of magnitude ($\approx 10^5$ sec⁻¹) for both glasses and crystals. Therefore, the condition $W_p \gg A$ for small energy gaps occurs more frequently in glasses. In this limit, the excited-state lifetime τ is given by $1/W_p$. The faster decay rates in glasses are an advantage, since when $W_p \gg A$, direct measurements of multiphonon rates are possible without the uncertainties associated with determining the radiative probabilities A in Eq. (12). The disadvantages are the low radiative quantum efficiency and the requirement of fast, sensitive photodetectors. Previous studies of multiphonon processes in glasses³ were limited to lifetimes greater than 1 μ sec. Here, we investigate lifetimes as short as 3 nsec.

B. Apparatus

Pulsed lasers are natural sources for selective excitation experiments. In these experiments, two laser systems with different pulse durations were employed. A schematic diagram of the apparatus is shown in Fig. 2. One system consisted

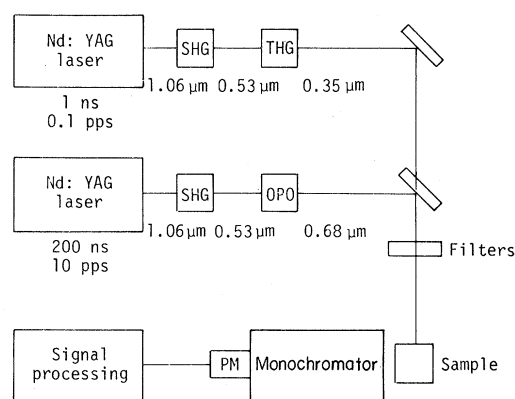


FIG. 2. Block diagram of experimental apparatus for transient fluorescence measurements. Second and third harmonic generating crystals (SHG and THG) and an optical parametric oscillator (OPO) were used to produce the desired pump wavelengths.

of a commercial (Chromatix) Q-switched Nd:YAG laser with a LiIO₃ frequency doubler (SHG) and a temperature-tuned LiNbO₃ optical parametric oscillator (OPO). This unit produced pulses at 10 pps with a duration of ~200 nsec. To generate shorter pulse durations needed for fast decay measurements, a synchronously Q-switched Nd:YAG oscillator¹⁹ was used. A Pockels cell driven by an optically triggered spark gap was used to select a single 1-nsec pulse which was then amplified to ~50 mJ. Second and third harmonics of the 1.064- μ m output were generated using KD*P doubler and mixing crystals to provide ~10-mJ pulses at 532 nm and ~1-mJ pulses at 355 nm.

Absorption or interference filters and a small grating monochromator were used to select the desired fluorescence wavelengths. To detect infrared fluorescence, a photomultiplier tube having an S-1 photocathode (Amperex 56 CVP) was used; for shorter-wavelength fluorescence, a tube with an S-20 response (Amperex 564 TUV) was used. The output was recorded with a Tektronix R7912 transient digitizer. The time resolution of the complete detection system was ~3 nsec. The signals were processed with a PDP-11/05 computer using programs developed for digital signal averaging, logarithmic plots of the transient fluorescence, and other data reduction.

To study the temperature dependence of multiphonon decay rates, the sample was placed in an electrically heated oven. A thermocouple in contact with the glass sample monitored the temperature. Samples could be heated to 800 K in this oven. Temperatures employed in the experiments were limited to <750 K to avoid softening the glasses.

C. Glass compositions

The glasses selected for study were simple three-component oxide glasses in which the network-forming complex was varied through the series: TeO₂, GeO₂, SiO₂, P₂O₅, B₂O₃. This series of glasses, as shown later, exhibits progressively higher vibrational frequencies. The base glass compositions are given in Table I and are identical

TABLE I. Base glass compositions in mol %.

	B ₂ O ₃	P ₂ O ₅	SiO ₂	GeO ₂	Na ₂ O	BaO
Borate	67				15	18
Phosphate		67			15	18
Silicate			67		15	18
Germanate				67	15	18
	TeO ₂	Al ₂ O ₃	WO ₃			
Tellurite	82	12	6			

except for the network former. The composition of the tellurite glass is different, however, because the sodium barium tellurite formulation did not form a stable glass. Rare-earth oxides (Nd, Er, Tm) were added in concentrations of <0.2 mol %, which were kept low to reduce non-radiative decay by ion-ion interactions. In some cases, both Er³⁺ and Tm³⁺ were present in the same sample, but this did not affect our measurements, since the energy levels of interest did not overlap.

The glasses, prepared at the National Bureau of Standards and Kigre, Inc., were melted in platinum crucibles and cast and annealed using standard glass forming techniques. Samples were polished with dimensions of several millimeters on a side.

D. Levels and decay schemes

Multiphonon decays measured in this work were restricted to those bridging energy gaps ranging from approximately 1400–4000 cm⁻¹. For smaller energy gaps, the decays were too fast to measure with the present apparatus, while for larger energy gaps, the multiphonon rates became small compared to radiative rates. Of the 13 trivalent rare earths, Nd³⁺, Er³⁺, and Tm³⁺ were studied. In Nd the decay across three energy gaps could be measured. In addition, the decay rates of Nd are of interest because of the importance of this ion for lasers. Erbium also provided three different energy gaps. Thulium provided a large energy gap which was well suited to temperature-dependence measurements.

The energy-level schemes, excitation and fluorescence transitions used, and the multiphonon decay rates measured for the three rare-earth ions are summarized in Fig. 3.

Energy gaps between *J* states were determined from absorption spectra of the ions in the glasses. Because of inhomogeneous broadening, assignments of energy gaps are imprecise but are believed to approximate the energy differences between the lowest Stark level of the emitting state to the highest Stark level of the terminal state. The energy gaps for a given ion did not vary significantly from glass to glass.

Neodymium. When Nd ions are excited by 532-nm radiation, the largest energy gap and hence the rate-limiting step in the nonradiative cascade to the ⁴F_{3/2} fluorescing level is that below the ⁴G_{7/2} level (energy gap 1400 cm⁻¹). When Nd ions are excited by 355-nm radiation, the ²P_{3/2} decay (energy gap 2200 cm⁻¹) is the rate-limiting step. The decay rates of both the ⁴G_{7/2} and ²P_{3/2} levels were determined from the risetime of the fluores-

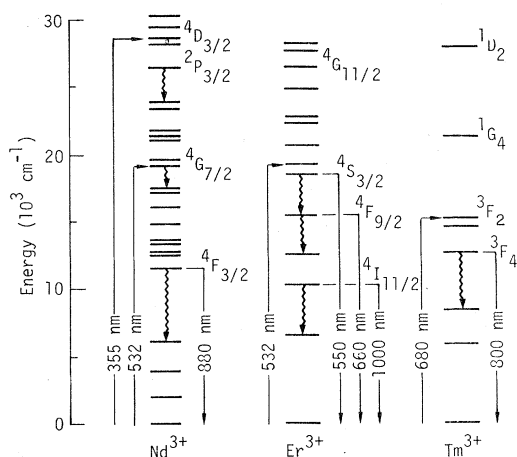


FIG. 3. Excitation and fluorescence schemes used to study multiphonon relaxation of rare earths. Wavy lines indicate nonradiative rates measured.

cence from ${}^4F_{3/2}$. These measurements were the most difficult to make and the least accurate. The early part of the fluorescence rise is distorted by the system response time and by any leakage of pump radiation into the photomultiplier. These problems combined with the low signal-to-noise ratio limited the fastest rates that could be measured confidently to about 10^8 sec^{-1} . The decay rates from ${}^2P_{3/2}$ and ${}^4G_{7/2}$ were not measurable in the borate and phosphate glasses, indicating that they were $\approx 10^8 \text{ sec}^{-1}$. The ${}^2P_{3/2}$ decay could not be measured in tellurite glass because the base glass strongly absorbs 355-nm radiation.

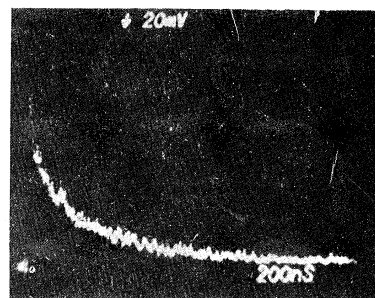
In borate glass, the Nd ${}^4F_{3/2}$ -level relaxation was faster than the radiative decay rate calculated by the Judd-Ofelt method²⁰ ($1.57 \times 10^4 \text{ sec}^{-1}$ vs $2.45 \times 10^3 \text{ sec}^{-1}$). The nonradiative rate was determined by subtraction using Eq. (12). In the other glasses, the nonradiative rates for the ${}^4F_{3/2}$ level (energy gap 4700 cm^{-1}) are much less than the radiative rate, resulting in large uncertainties when the calculated radiative rates are subtracted to determine the multiphonon rates. Within experimental error, the multiphonon rates for ${}^4F_{3/2}$ are consistent with extrapolations of the exponential energy gap dependence (see Fig. 6).

Erbium. The three energy gaps of Er that were studied are shown in Fig. 3. After excitation with 532-nm pump radiation, the ions rapidly relax to the ${}^4S_{3/2}$ level, which exhibits an exponential decay across a gap of about 2800 cm^{-1} . Although this decay is predominantly nonradiative, there is still sufficient radiative quantum efficiency to observe ${}^4S_{3/2}$ fluorescence. The ${}^4F_{9/2}$ level immediately below the ${}^4S_{3/2}$ level decays faster than ${}^4S_{3/2}$ since it has a smaller gap below it (2600 cm^{-1}). Thus, the ${}^4F_{9/2}$ fluorescence signal rises to a peak inten-

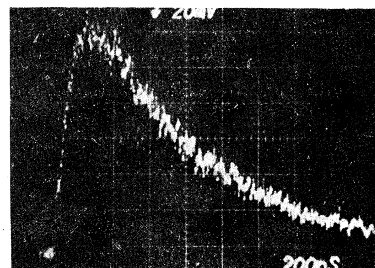
sity as it is fed by ${}^4S_{3/2}$ and then decays with a rate that approaches that of ${}^4S_{3/2}$ at long times. Examples of the transient fluorescence from the ${}^4S_{3/2}$ and ${}^4F_{9/2}$ states of Er^{3+} in a silicate glass are shown in Fig. 4. The decay of the ${}^4I_{11/2}$ level across a gap of $\sim 3300 \text{ cm}^{-1}$ was slow enough that the rise of the 1- μm fluorescence was effectively instantaneous when recorded on a time scale appropriate to the decay.

Thulium. The Chromatix laser-optical parametric oscillator operating at 680 nm was used to excite Tm into the 3F_2 state from which it relaxed rapidly to the 3F_4 . Emission at 800 nm was observed as a monitor of the 3F_4 population. The uncertainty in determining the energy gap for this transition was large due to the unusually broad 3F_4 and 3H_5 absorption bands. A value of 3800 cm^{-1} was used. The total decay rate of the 3F_4 level in germanate and tellurite glasses was small enough that the radiative contribution could not be ignored. Reisfeld and Eckstein²¹ have calculated the radiative intensity parameters for Tm^{3+} in germanate and tellurite glasses. Using these values combined with calculated matrix elements, the radiative rates from 3F_4 for the two glasses were estimated. Although the glass compositions

550 nm Emission



200 ns



660 nm Emission

FIG. 4. Fluorescence from excited states of Er^{3+} in silicate glass following pulsed excitation at 532 nm. Top: emission from ${}^4S_{3/2}$ at 550 nm; bottom: emission from ${}^4F_{9/2}$ at 660 nm.

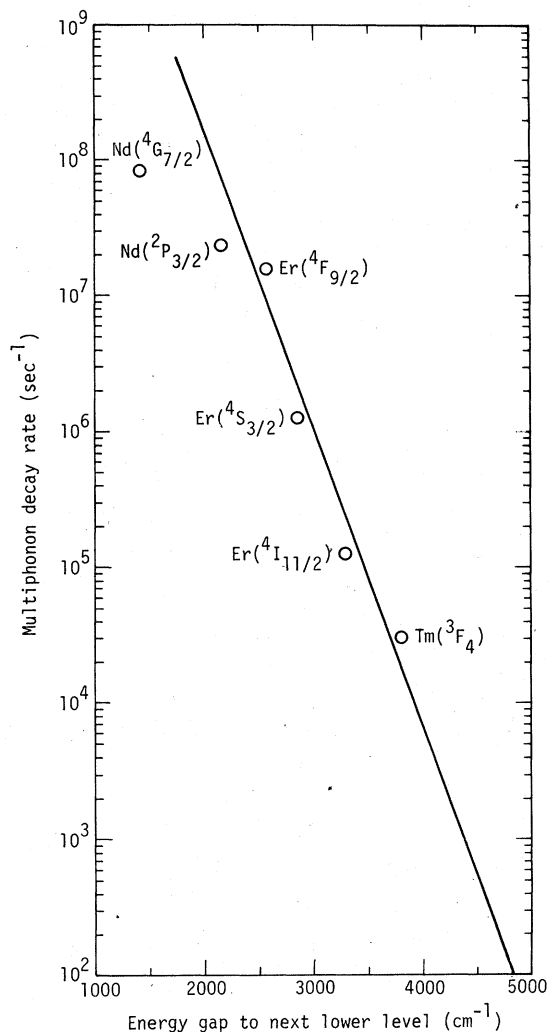


FIG. 5. Multiphonon decay rates for rare-earth ions in silicate glass plotted as a function of energy gap to the next-lower level. Ions and excited states measured are indicated.

were not identical to those of Reisfeld and Eckstein, the estimates are probably accurate to $\pm 30\%$. The predicted radiative rate in germanate is 880 sec^{-1} , and in tellurite is $2.2 \times 10^3 \text{ sec}^{-1}$. These rates were subtracted from the observed total decay rates to give the multiphonon rates. The total decay rates in silicate, phosphate, and borate glasses were greater than $3 \times 10^4 \text{ sec}^{-1}$, and no radiative correction was made.

IV. RESULTS

A. Dependence on energy gap

The measured nonradiative decay rates in silicate glass at room temperature are plotted semi-logarithmically versus energy gap to the next-

lower ionic energy level in Fig. 5. These results and those presented below were all obtained by fitting the observed fluorescences to simple exponential time dependences. The signal-to-noise ratios were not sufficient to warrant consideration of the multiexponential behavior arising from site variations in glass noted in the Introduction. With the exception of one point at 1400 cm^{-1} , the decay rates for six energy levels of the three ions studied follow the simple exponential dependence on the energy gap given by Eq. (11). This behavior confirms the main assumption of the multiphonon relaxation theory that the terms of the perturbation expansion converge rapidly and that, for high-order processes, the rate depends on the energy gap and not on the particular ion, energy level, or vibrational mode involved in the decay. These results are in agreement with our earlier investigation of multiphonon relaxation in a complex silicate glass.²¹ The measured rate for decay from the ${}^4G_{7/2}$ level of Nd falls below the value which would be predicted from the 1400-cm^{-1} energy gap. However, as shown later, this decay corresponds to only a one- or two-quanta excitation of the network normal mode. In this case, the multiphonon theory does not apply since the decay rate depends on the specific energy level and its coupling to the glass network.

In Fig. 6, the nonradiative decay rates measured

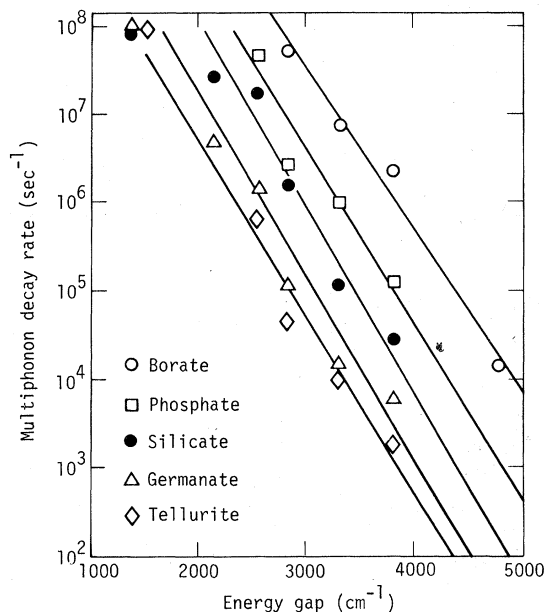


FIG. 6. Multiphonon decay rates for rare-earth ions in five oxide glasses plotted as a function of the energy gap to the next-lower level. The approximate frequencies of the high-energy phonons in each glass are: borate— 1350 cm^{-1} ; phosphate— 1100 cm^{-1} ; silicate— 1000 cm^{-1} ; germanate— 900 cm^{-1} ; and tellurite— 800 cm^{-1} .

in each of the five oxide glasses are plotted on a semilogarithmic scale versus energy gap. The rates for each glass follow the simple exponential dependence on energy gap. We find, in addition, a strong dependence of the rates on the host glass composition. The fastest decays occur in borate glass, followed in order by phosphate, silicate, germanate, and tellurite. For each level the decay rate in tellurite glass is approximately 10^{-3} times the corresponding rate in borate glass, yet the rates in tellurite are ten times greater than the fastest measured rates in crystal host materials.¹

Multiphonon decay rates for the $^4S_{3/2}$ and $^4F_{9/2}$ levels of Er in germanate and tellurite glasses have also been determined by Reisfeld and Eckstein,²² using a different technique. They measured the fluorescence quantum efficiency and lifetimes, and then derived the nonradiative rate from Eq. (13) using radiative rates calculated by the Judd-Ofelt technique. Although their result for the $^4S_{3/2}$ decay rate in germanate glass agrees with our measurement, their other rates are approxi-

mately five times less than those shown in Fig. 6. In addition, Reisfeld *et al.*^{3,23} obtained values for the Tm 1D_2 to 1G_4 decay across an energy gap of 6300 cm^{-1} in borate, phosphate, and germanate glasses. Their results are 10^2 greater in borate and more than 10^3 greater in phosphate and germanate than those obtained from extrapolation of the exponential dependences in Fig. 6. Such differences can result from uncertainties in Judd-Ofelt calculations, which become significant when the radiative rate is comparable to the nonradiative rate.

B. Dependence on glass network former

Understanding the decay rate dependence on the glass host composition requires knowledge of the glass network vibrational frequencies which are excited in the decay. These frequencies can be determined from Raman spectra. Shuker and Gammon²⁴ and Brawer¹² have shown that the complete vibrational spectrum in glasses can be determined from the first-order Raman scattering intensity. Spontaneous Raman spectra of the glasses studied are shown in Fig. 7.²⁵ For each glass, the highest-frequency vibration is associated with the symmetric stretching mode of the glass network former.²⁶ The approximate center frequency of this highest energy band for each glass is included in the caption of Fig. 6. With reference to Fig. 6, the decay rate for each level varies among the glasses in the same order as the energy of the highest-frequency vibration. This result strongly suggests that the nonradiative decay in glasses, as in crystals, occurs predominantly by excitation of the highest-frequency vibrations of the glass network.

C. Dependence on temperature

To investigate this issue, the measured temperature dependence of the rate for the $^3F_4 \rightarrow ^3H_5$ decay in Tm was fit by the expression given in Eq. (11). This procedure allows both the order of the decay process and the frequency of the network vibration excited in the decay to be determined. Three constraints were applied in the fitting. First, only integer values for the order p were used; second, the vibrational frequencies were chosen to be at or near peaks in the Raman spectra; and third, energy was conserved in the decay. The calculated temperature dependence for a four- and a five-phonon decay in silicate glass are given in Fig. 8, along with the measured rates. Comparison of the temperature dependences for the four- and five-phonon decays show the sensitivity of this curve-fitting procedure. The better fit is obtained for a five-phonon decay and the cor-

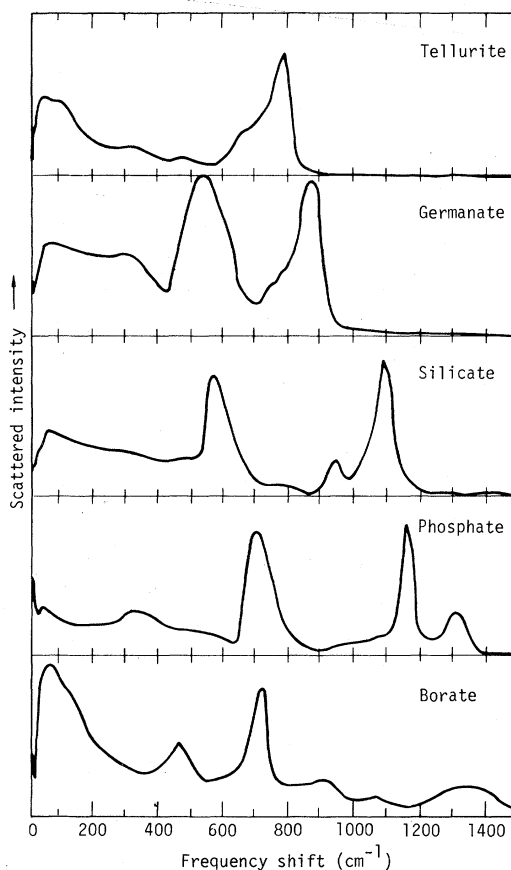


FIG. 7. Polarized Raman spectra of oxide glasses used for multiphonon relaxation studies.

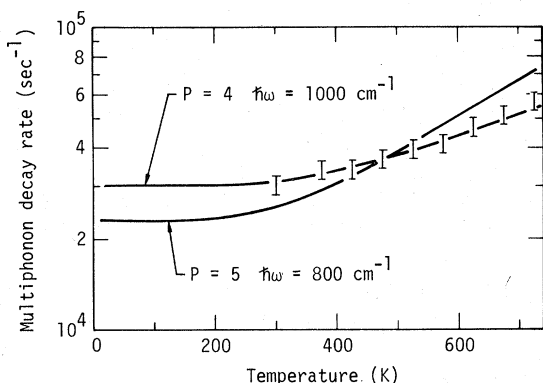


FIG. 8. Temperature dependence of the ${}^3F_4 \rightarrow {}^3H_5$ multiphonon emission rate for Tm^{3+} in silicate glass. Two fits of the data using Eq. (11) are shown.

responding phonon energy of 1000 cm^{-1} falls in the highest-frequency Raman band. Although it is clear that the high-energy phonons are active in the decay, it is not possible to definitely assign the decay to a particular phonon energy, and this result should be interpreted only in a qualitative sense. For example, a four-phonon decay involving either 900- or 1100-cm^{-1} phonons fits as well. The restriction of p to integer values determines the phonon energy if the energy gap is known; however, the gap for the same ion in different sites may vary and hence is not known accurately. Three phonons of one energy and one of another energy also have been fitted, but the results are no more definitive than for the single-frequency model shown. In addition, the high-energy peaks in the Raman spectra consist of more than one type of vibration. In the simple silicate, there is evidence for an unresolved peak at about 1025 cm^{-1} between the two large peaks at 1100 and 950 cm^{-1} . The depolarized Raman spectrum shows this peak more clearly, since the strongly polarized peaks at 1100 and 950 cm^{-1} are very weak in the depolarized spectrum. Thus, there are at least three high-energy peaks in the silicate glass which may be active in multiphonon relaxation, but the energies are too similar to differentiate their relative importance by these temperature-dependence measurements. In the absence of information about the site occupied by the rare-earth ion or the coupling of the ion in glasses, the active vibration cannot be predicted. It is clear from these results that phonons of approximately 1000 cm^{-1} are responsible for the multiphonon decay. The order of the process, if not the exact phonon energy, is evident from the temperature dependence.

Figure 9 shows the best fit for the Tm decays in phosphate, silicate, germanate, and tellurite glasses. The Tm decay in borate showed varia-

tion with temperature that was less than the experimental error, consistent with the low order of the process using 1400-cm^{-1} phonons. For the germanate and tellurite glasses, the calculated radiative rates were included in the theoretical curves.

Riseberg⁶ and Reed²⁷ have introduced into the temperature dependence the depletion of the decaying level by thermal population of higher-lying levels of arbitrary degeneracy which are assumed to be nondecaying. This latter assumption is not justified in the present case since the energy gap for these thermally populated levels is not significantly greater than for the decaying level itself, and multiphonon theory predicts that the energy gap alone determines the decay rate.

V. CONCLUSION

Based on measured decay rates, we have shown that the theory of multiphonon relaxation adequately describes nonradiative relaxation of excited rare-earth ions in oxide glasses. The predicted exponential dependence of relaxation rate on energy gap was observed in all five glasses, justifying

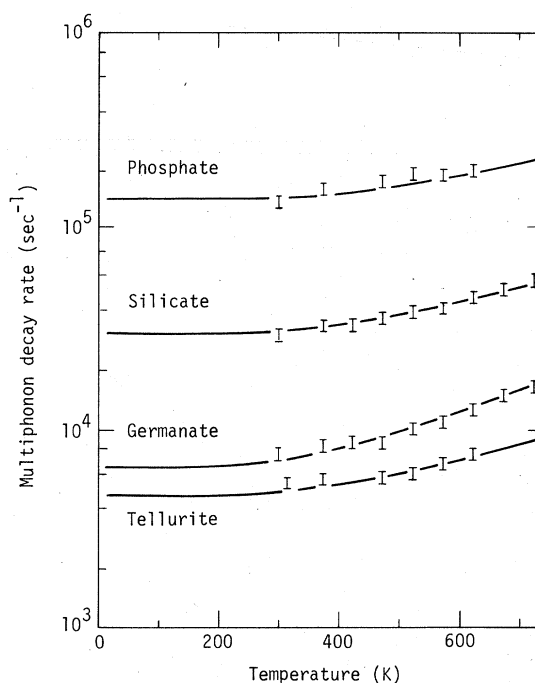


FIG. 9. Comparison of the temperature dependences of the ${}^3F_4 \rightarrow {}^3H_5$ multiphonon emission rates for Tm^{3+} in four different oxide glasses. The curves are temperature dependences predicted from Eq. (11) using the following numbers and energies of phonons: phosphate glass—4 phonons, 1100 cm^{-1} ; silicate glass—4 phonons, 1000 cm^{-1} ; germanate glass—5 phonons, 825 cm^{-1} ; tellurite glass—5 phonons, 760 cm^{-1} .

the perturbation expansion approach that leads to Eq. (11). The importance of only the highest-energy vibrations is further confirmed by the observed increase of multiphonon rate with increasing temperature, in agreement with the temperature dependence of the occupation numbers of the highest-energy modes in each of the glasses. The variation of multiphonon rates with glass network former correlates with the highest available phonon energy in the glasses, with the rates in borate glass exceeding the analogous rates in tellurite by 10^3 . No instance was observed where the ion-phonon coupling strength in one glass differed from the other glasses enough to overcome the dominant influence of phonon energies in determining the relative multiphonon rates. Thus, the coupling strengths appear to be approximately equal for the five glasses studied. Deviations from the ordering of multiphonon rates according to maximum phonon energies are possible for glass network formers other than oxides (for instance, halides or chalcogenides).

These results provide the most sensitive test to date of the applicability of multiphonon theory to glasses. These multiphonon rates were measured directly, avoiding the uncertainty associated with subtracting calculated radiative rates from observed total decay rates. The outcome of this test of the theory indicates that multiphonon relaxation in glasses is characterized by the same processes as in crystals and is well described by the theory developed for crystals.

ACKNOWLEDGMENTS

We thank D. Downs and R. Morgret for their excellent technical assistance during these experiments. The tellurite glass was prepared by J. D. Myers of Kigre, Inc.; all other glasses were melted by D. Blackburn of the National Bureau of Standards. We are grateful to R. C. Harney and F. P. Milanovich of LLL for recording the Raman spectra. One of us (C.B.L.) acknowledges helpful discussion of multiphonon relaxation with R. Orbach.

*Work performed under the auspices of the U. S. ERDA, Contract No. W-7405-ENG-048.

¹L. A. Riseberg and M. J. Weber, in *Progress in Optics*, edited by E. Wolf (North-Holland, Amsterdam, 1976), Vol. 14, p. 89.

²M. J. Weber *et al.*, *J. Lumin.* **12**, 729 (1976); C. Brecher and L. A. Riseberg, *Phys. Rev. B* **13**, 81 (1976).

³R. Reisfeld, in *Structure and Bonding*, edited by J. D. Dunitz *et al.* (Springer, Berlin, 1975), Vol. 22, p. 123; R. Reisfeld *et al.*, *J. Lumin.* **10**, 193 (1975).

⁴B. R. Judd, *Phys. Rev.* **127**, 750 (1962); G. S. Ofelt, *J. Chem. Phys.* **37**, 511 (1962).

⁵A. Kiel, Ph.D. thesis (Johns Hopkins University, 1962) (unpublished); A. Kiel, in *Paramagnetic Resonance*, edited by W. Low (Academic, New York, 1963), p. 525.

⁶L. A. Riseberg and H. W. Moos, *Phys. Rev.* **174**, 429 (1968).

⁷T. Miyakawa and D. L. Dexter, *Phys. Rev. B* **1**, 2961 (1970).

⁸S. Fischer, *J. Chem. Phys.* **53**, 3195 (1970).

⁹F. K. Fong, *Theory of Molecular Relaxation* (Wiley, New York, 1975).

¹⁰C. W. Struck and W. H. Fonger, *J. Lumin.* **10**, 1 (1975).

¹¹H. Rawson, *Inorganic Glass-Forming Systems* (Academic, New York, 1967), p. 11.

¹²S. Brawer, *Phys. Rev. B* **11**, 3173 (1975).

¹³R. J. Bell and P. Dean, *Nature* **212**, 1354 (1966); R. J. Bell, N. F. Bird, and P. Dean, *J. Phys. Chem.* **1**, 299 (1968); R. J. Bell and D. C. Hibbins-Butler, *ibid.* **8**, 787 (1975).

¹⁴J. Bock and G. J. Su, *J. Am. Ceram. Soc.* **53**, 69

(1970); N. F. Borrelli and G. J. Su, *Phys. Chem. Glasses* **4**, 206 (1963).

¹⁵J. B. Bates, *J. Chem. Phys.* **56**, 1910 (1972).

¹⁶C. B. Layne, Ph.D. thesis (University of California, 1975) (unpublished).

¹⁷K. R. German and A. Kiel, *Phys. Rev. B* **8**, 1846 (1973).

¹⁸S. A. Pollack, *J. Chem. Phys.* **38**, 2521 (1963); **40**, 2751 (1964); M. J. Weber, *Phys. Rev.* **156**, 231 (1967).

¹⁹R. L. Carman, B. C. Johnson, and L. L. Steinmetz, *Opt. Commun.* **7**, 169 (1973); see also Ref. 16.

²⁰R. R. Jacobs and M. J. Weber, *IEEE J. Quantum Electron.* **QE-12**, 102 (1976).

²¹C. B. Layne, W. H. Lowdermilk, and M. J. Weber, *IEEE J. Quantum Electron.* **QE-11**, 798 (1975).

²²R. Reisfeld and Y. Eckstein, *J. Non-Cryst. Solids* **15**, 125 (1974).

²³R. Reidfeld and Y. Eckstein, *J. Chem. Phys.* **63**, 4001 (1975).

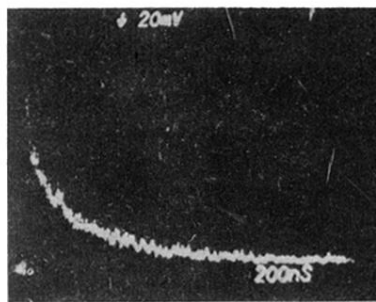
²⁴R. Shuker, Ph.D. thesis (Catholic University, Washington, D.C., 1971) (unpublished); R. Shuker and R. W. Gammon, *Phys. Rev. Lett.* **25**, 222 (1970).

²⁵The Raman spectra were derived from data provided by R. C. Harney and F. P. Milanovich. For a description of their apparatus see R. C. Harney and F. P. Milanovich, *Rev. Sci. Instrum.* **46**, 1047 (1975).

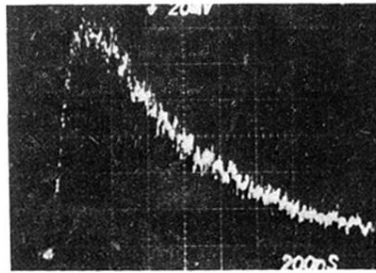
²⁶I. Simon, in *Modern Aspects of the Vitreous State*, edited by J. D. Mackenzie (Butterworths, London, 1960), p. 120.

²⁷E. D. Reed, Jr., and H. W. Moos, *Phys. Rev. B* **8**, 980 (1973); E. D. Reed, Jr., Ph.D. thesis (Johns Hopkins University, 1972) (unpublished).

550 nm Emission



—| |← 200 ns



660 nm Emission

FIG. 4. Fluorescence from excited states of Er^{3+} in silicate glass following pulsed excitation at 532 nm. Top: emission from ${}^4\text{S}_{3/2}$ at 550 nm; bottom: emission from ${}^4\text{F}_{9/2}$ at 660 nm.